TISSUE ENGINEERING: Part A
Volume 18, Numbers 1 and 2, 2012

DOI: 10.1089/ten.tea.2011.0231

Three-Dimensional Engineered Bone–Ligament–Bone Constructs for Anterior Cruciate Ligament Replacement

Jinjin Ma, M.S.,[1] Michael J. Smietana, M.S.,[2] Tatiana Y. Kostrominova, Ph.D.,[3] Edward M. Wojtys, M.D.,[4] Lisa M. Larkin, Ph.D.,[2,5] and Ellen M. Arruda, Ph.D.[1,2,6]

The anterior cruciate ligament (ACL), a major stabilizer of the knee, is commonly injured. Because of its intrinsic poor healing ability, a torn ACL is usually reconstructed by a graft. We developed a multi-phasic, or bone–ligament–bone, tissue-engineered construct for ACL grafts using bone marrow stromal cells and sheep as a model system. After 6 months *in vivo*, the constructs increased in cross section and exhibited a well-organized microstructure, native bone integration, a functional enthesis, vascularization, innervation, increased collagen content, and structural alignment. The constructs increased in stiffness to 52% of the tangent modulus and 95% of the geometric stiffness of native ACL. The viscoelastic response of the explants was virtually indistinguishable from that of adult ACL. These results suggest that our constructs after implantation can obtain physiologically relevant structural and functional characteristics comparable to those of adult ACL. They present a viable option for ACL replacement.

Introduction

Knee injuries accounted for 400,000 physician office visits in the United States in 2005.[1] Worldwide, the proportion of knee injuries to young sports players that require surgery is estimated to be 17%–61%,[2] and in the United States, knee injuries are now the leading cause of high school sports-related surgeries.[3] In addition to the high costs associated with the surgery itself, acute knee injury is a risk factor for osteoarthritis (OA).[4–6] Anterior cruciate ligament (ACL) reconstruction surgeries, involving bone/ligament autografts or allografts, are performed in the United States at a rate of nearly 350,000 per year and acute care alone requires for $6 billion annually.[7] Current knee ligament replacement strategies involve either ACL allografts from cadavers or autografts of the patients' own patellar or hamstring tendons. Outcomes for ACL reconstruction with these techniques are limited by graft availability, risk of rejection, and increased donor site morbidity. In addition, the region of the graft or engineered material within the bone tunnel may not fully integrate with native tissue.[8,9] The initial response of the body to either grafts or current tissue engineering approaches results in reduced stiffness of the replacement.[10] Many grafts function as mechanical springs that span the gap between the femur and tibia, providing stability and allowing joint motion, but do not complete the ligamentization process or restore the original biomechanics to the knee even 2–3 years after surgery.[8–10] In addition, the incidence of early-onset OA within 7–14 years after knee injury is as high as 50%,[5,11,12] without improved outcomes as a result of ACL reconstruction.[5,13] Thus, there is a need for a ligament graft that will develop biochemically relevant and biomechanically compatible interfaces with native tissue and restore the proper biomechanics and physiological function to the ligament. We have developed a multi-phasic engineered bone/ligament co-culture with a viable bone–ligament interface *in vitro* and the capacity to develop vascular and neural systems[14,15] in sheep that may greatly expand the potential for ligament repair by providing a functional enthesis between the engineered ligament and bone and the potential to reestablish the ACL-hamstring reflex arc.

Autografts are the current gold standard for ACL replacements and the patellar tendon is the most common source of autograft tissue. However, the viscoelastic properties of the patellar tendon differ in several important ways from those of the ACL. The initial stiffness of the patellar tendon exceeds that of the ACL,[16,17] patellar tendon strain to failure at a given strain rate is significantly less than that of ACL, which may lead to increased failure incidences[16,17] and

Departments of [1]Mechanical Engineering and [2]Biomedical Engineering, University of Michigan, Ann Arbor, Michigan.
[3]Department of Anatomy and Cell Biology, Indiana University School of Medicine-Northwest, Gary, Indiana.
[4]Medsport Sports Medicine Program, Department of Orthopaedic Surgery, University of Michigan, Ann Arbor, Michigan.
[5]Department of Molecular and Integrative Physiology, University of Michigan, Ann Arbor, Michigan.
[6]Program in Macromolecular Science and Engineering, University of Michigan, Ann Arbor, Michigan.

the patellar tendon failure strain is more sensitive to strain rate than the ACL failure strain; at higher strain rates the failure strain for the patellar tendon decreases rapidly, again leading to increased failure risks under impact loads. Therefore, an engineered ligament that has the capacity to develop the viscoelastic properties of the native ACL would be an improvement over currently used patellar tendon grafts. The compliance mismatch and dissimilar tissue interface between native bone and engineered ligament are additional existing design limitations that may impede translation to clinical applications.[18,19]

These limitations have led investigators to develop strategies to engineer ligament tissue to reduce or eliminate the need for graft tissue altogether.[20] Current tissue engineering approaches usually involve seeding cells onto a natural or synthetic scaffold that is both biocompatible and degradable.[21] Typically, the scaffold, initially mimicking the structural and mechanical properties of the ACL, gradually degrades and transfers the mechanical loads to the new tissue regenerated within the scaffold. The incorporation of growth factors has been used to enhance cell migration, proliferation, and collagen deposition in ACL repair. For a detailed review of biomaterials and scaffold designs, and growth factors currently utilized in engineering ligament tissue, refer to the following reviews.[20–23] In the approach taken here, isolated bone marrow stromal cells (BMSCs) are differentiated along osteogenic and fibrogenic pathways and in doing so, generate their own extra-cellular matrices. These matrices are then manipulated by the cells via contraction to form the constructs without artificial scaffolds. The resulting three-dimensional (3D) multi-phasic bone–ligament–bone (BLB) constructs exhibit the structural and functional interface characteristics of native ACL by utilizing engineered ligament with engineered bone at each end. We hypothesize that the BLB constructs can integrate into the recipient bone to form a mechanically viable and biochemically relevant interface between the two tissues and allow rapid growth of the BLB construct to attain mechanical and histological properties that resemble those of native, adult ACL.

BMSC create an environment that diminishes immune response and enhances regeneration. Thus, the potential to use allogenic sources rather than autogenic sources of BMSC exists.[24] BMSCs can be easily isolated from autologous sources, may be expanded in culture while maintaining their multipotency, and therefore serve as an attractive candidate for tissue engineering.[24–29] BMSCs also secrete bioactive factors that inhibit scarring and apoptosis and stimulate angiogenesis.[24] BMSCs are an accessible and biocompatible source of cells that are immunosuppressive, especially for T-cells,[24] making both autogenic and allogenic sources good candidates for use in regenerative medicine. The *in vitro* BLB constructs that we have developed are made with BMSCs as a cell source and consist of differentiated ligament tissue in the middle and differentiated bone tissue on the ends.[14,15]

The purpose of this study was to engineer a 3D multiphasic ligament model or BLB construct that will rapidly grow and remodel *in vivo* to attain biomechanical properties of native ACL. We used these BLB constructs as ACL replacements in sheep, explanted them at 2, 3, 4, and 6 months and characterized their mechanics and histology.

Methods

Animal model and animal care

Black Suffolk female sheep were used as hosts and BMSC donors for the fabricated BLB constructs. The sheep and goat have commonly been chosen as animal models for the knee[30–33] because of anatomical[34–37] and mechanical[38–41] similarities to human ACLs. These sheep were obtained from the Michigan Livestock Exchange, various farms in the area or intra-university transfer. All animals were acclimated to our Sheep Research Facility at the University of Michigan for 1 week before any procedure. Sheep were allowed to free range in the pasture until used for surgical implantation. The animals were given access to food and water ad libitum. Femur and tibia bones were surgically dissected under aseptic conditions from the sheep immediately after euthanasia with Fatal Plus (Vortech Pharmaceuticals), to obtain bone marrow for BLB construct fabrication. The BLB constructs were implanted into the ACL site as a replacement tissue and the animals were allowed to recover for 2, 3, 4, or 6 months before explantation. All surgical procedures were performed in an aseptic environment with anesthesia induced by intravenous injections of Ketamine and Diazepam and sustained with inhalation of halothane gas. After any surgical procedure, the animals were singly housed in secluded pens for 2 weeks and then released back into the herd until the date of explantation. All animal care and animal surgeries were in accordance with The Guide for Care and Use of Laboratory Animals (Public Health Service, 1996, NIH Publication No. 85-23); the experimental protocol was approved by the University Committee for the Use and Care of Animals.

Preparation of solutions and media

Unless otherwise indicated, all solutions and media were prepared and stored at 4°C before isolation and culture of BMSC and warmed to 37°C in a heated water bath immediately before use. The media, with slight modifications from Ref.[14], were as follows: ligament growth medium (GMA) consisted of 400 mL Dulbecco's modified Eagle's medium (DMEM) with 100 mL fetal bovine serum (Gibco BRL), 6 ng/mL basic fibroblast growth factor (bFGF; Peprotech), 0.13 mg/mL asc-2-phos, 0.05 mg/mL L-proline, and 5 mL A9909 (Sigma A9909), and differentiation medium (DMA) consisted of 460 mL DMEM with 35 mL 100% horse serum albumin (Gibco BRL), 0.13 mg/mL asc-2-phos, 0.05 mg/mL L-proline, 2 ng/mL transforming growth factor beta (Peprotech), and 5 mL A9909 (Sigma). For bone, the growth medium and the differentiation medium were the same GMA and DMA as ligament with the addition of 10^{-8} M dexamethasone (DEX; Sigma-Aldrich).

Preparation of culture dishes

BLB constructs were engineered in individual 100 mm cell culture plates following a slightly modified protocol previously developed.[14] Briefly, plates were coated with 12.0 mL of Sylgard (Dow Chemical Corporation, type 184 silicon elastomer) and allowed to cure for 3 weeks before use. These Sylgard-coated dishes were used for fabricating 3D constructs as described in detail in the following two sections. Each of these plates was then filled with 16 mL of 25 mL of

Dulbecco's phosphate-buffered saline (DPBS) pH 7.2 ([Gibco BRL Cat# 14190-144] per plate) and decontaminated with UV light (wavelength 253.7 nm) for 90 min and placed in a 37°C 5% CO_2 incubator for 1 week before use.

Bone marrow stem cell isolation and expansion

Femur and tibia bones were surgically removed under aseptic conditions from both legs. The surrounding soft tissue was dissected and the proximal end of the femur and distal end of the tibia were cut to expose the marrow. The marrow was scooped using a spatula into a 50 mL conical filled with DMEM (Gibco). The BMSCs were isolated and expanded according to a protocol developed in our lab with some slight modifications.[14] The marrow was minced with scissors, vortexed, and pelleted using centrifugation (AccuSpin FR; Beckman Coulter, Inc.) at 1000 rpm for 5 min at 25°C. The supernatant was removed using aspiration. The total mass of the bone marrow was measured. Then, the marrow was resuspended in 8 mL GMA (previously described) in 100-mm-diameter tissue culture dishes with 0.06 g of bone marrow per ligament dish on average and 0.03 g of bone marrow per bone dish on average. Eighty microliters of bFGF was added to each bone dish and ligament dish. Eighty microliters of DEX was added to each bone dish additionally. The dishes were incubated at 37°C, 95% humidity, and 5% CO_2. After 48 h, the nonadherent cells were removed by feeding the plates with fresh GMA (as appropriate for constructs under construction; ligament or bone). The adherent BMSC were cultured to 80% confluence, at which time cells were enzymatically removed from the 100 mm plate using a 0.25% trypsin–ethylenediaminetetraacetic acid solution (Gibco) and passaged. Cells were plated onto construct dishes within the third and fifth passages.

Preparation of self-organized bone constructs

Bone constructs were engineered following a previously developed protocol.[42] After incubation, the GMA was aspirated and 2×10^5 cells, suspended in 16 mL bone GMA, and were seeded onto 35 mm cell culture plates. The medium was changed every 2–3 days. When the cells became confluent, after approximately 5 days, DMA was substituted for GMA to induce construct formation. After approximately 2 days, a bone monolayer was formed on each dish. The monolayers were carefully transferred from the current culture dishes to Sylgard-coated dishes using sterilized tweezers. Two minutien pins were placed on the monolayers approximately 20 mm apart in the dish to guide the assembly of 15–20 mm long bones. The differentiation medium was changed every 2–3 days until the constructs were used for co-culturing BLB constructs.

BLB construct formation

Eight milliliters of the cell suspension containing 2×10^5 cells/mL of ligament GMA was plated in each 100 mm culture dish. The dishes were then placed in a 37°C 5% CO_2 incubator and the medium was changed every 2–3 days. After the cells become confluent, approximately three days later, a ligament monolayer had formed on each 100 mm culture dish. The monolayers were carefully transferred to Sylgard-coated dishes (as described above) with sterilized tweezers. Engineered bones (fabricated as described above) of approximately 15–20 mm in length were pinned, using two minutien pins, on top of the ligament monolayer, and in-line axially so that the inner ends were 30–40 mm apart to fabricate a 60–80 mm long BLB. At this point DMA replaced GMA. The individual BLB constructs had a diameter of 0.6 to 0.8 mm. Within 1 week of implantation eight of these constructs were pinned together laterally at their bone ends to form a larger width construct with dimensions of approximately 60 to 80 mm long, 2.8–3.2 mm in diameter. This large lamellar construct fused together laterally before implantation and was of sufficient size for implantation as a sheep ACL replacement. The BLB constructs did not develop a necrotic core during this period of time *in vitro*.

The entire fabrication process is shown schematically in Figure 1. BMSCs were first isolated from sheep femurs (Step 1). Cells were proliferated and differentiated into bone-like cells and ligament-like cells using growth media and growth factors (Step 2). Bone cells were seeded onto 35 mm cell culture plates. Cells became confluent and a bone monolayer was formed on each dish (Step 3). Ligament cells were seeded onto 100 mm cell culture plates. In the same fashion, cells became confluent and a large ligament monolayer was formed on each dish (Step 4). The bone monolayers were transferred from the culture dishes to Sylgard-coated dishes with two minutien pins placed on each monolayer approximately 20 mm apart to guide the formation of 3-D bone constructs (Step 5). The ligament monolayers were carefully transferred to Sylgard-coated 100 mm dishes. Two of the engineered 3D bone constructs were pinned on top of a ligament monolayer, and in-line axially so that the inner ends of the bone constructs were 30–40 mm apart, to fabricate a 60–80 mm long BLB (Step 6). Within 1 week before implantation eight of these constructs were pinned together laterally at their bone ends. Constructs fused together laterally to form a larger width construct with dimensions of approximately 60–80 mm long, 2.8–3.2 mm in diameter (Step 7). The BLB constructs did not develop a necrotic core during this period of time *in vitro*. The BLB constructs were then used for implantation as a sheep ACL replacement (Step 8).

Replacement of the ACL with engineered BLB constructs in sheep

Before ACL reconstruction surgery, the sheep was placed supine on the operating table. General anesthesia was administered for ACL reconstruction. The surgical site was prepared by shaving the wool, washing dirt, and debris from the site and surgically scrubbing with povidone iodine soap followed by multiple applications of Betadine. Sterile ophthalmic ointment was applied to the eyes. The body temperature was maintained by placing the animal on a heat pad and covering it with a blanket and was monitored with a rectal thermometer. A 1-inch medial para patellar tendon arthrotomy was used to expose the intercondylar notch and excise the fat pad after 5 mL of Marcaine 1% with 1:200,000 epinephrine had been injected for hemostasis. The ACLwas then excised leaving a remnant of the ACL stump on both the femur and tibia to aid in positioning the ACL graft. The tibial tunnel entrance was placed on the metaphyseal flare just anterior to the medial collateral ligament and medial to the tibial tuberosity. This medial site allowed oblique

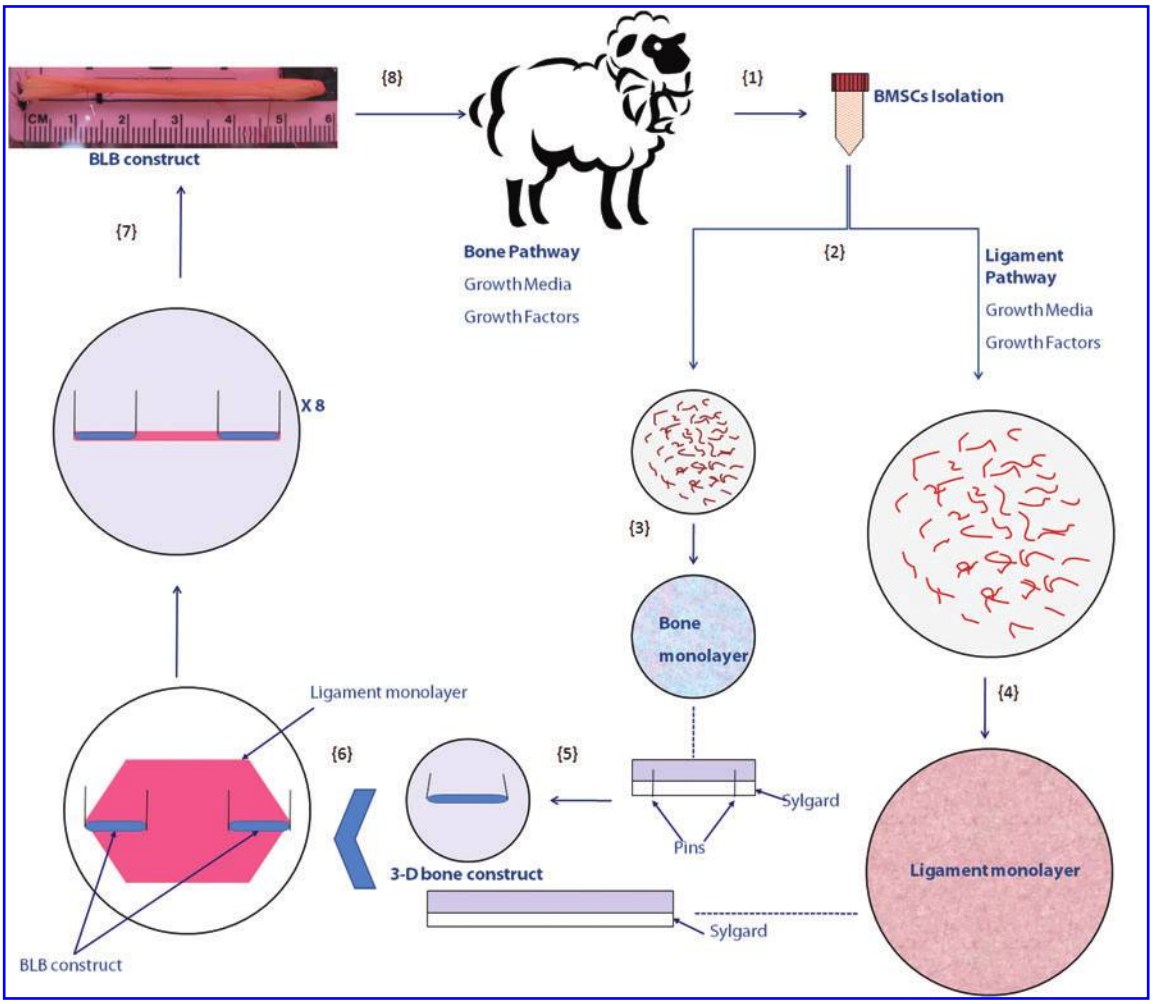

FIG. 1. Fabrication process of a BLB construct *in vitro*. BMSCs were first isolated from sheep femurs (Step 1). Cells were proliferated and differentiated into bone-like cells and ligament-like cells using growth media and growth factors (details can be found in the Methods Section Step 2). Bone cells were seeded onto 35 mm cell culture plates. Cells became confluent and a bone monolayer was formed on each dish (Step 3). Ligament cells were seeded onto 100 mm cell culture plates. In the same fashion, cells became confluent and a large ligament monolayer was formed on each dish (Step 4). The bone monolayers were transferred from the current culture dishes to Sylgard-coated dishes with two minutien pins placed on each monolayer approximately 20 mm apart to guide the formation of a 3D bone construct (Step 5). The ligament monolayers were carefully transferred to Sylgard-coated 100 mm dishes. Two of the engineered 3D bone constructs were pinned on top of a ligament monolayer, and in-line axially so that the inner ends of the bone constructs were 30–40 mm apart, to fabricate a 60–80 mm long BLB (Step 6). Within 1 week of implantation eight of these constructs were pinned together laterally at their bone ends. Constructs fused together laterally to form a larger width construct with dimensions of approximately 60–80 mm long, 2.8–3.2 mm in diameter (Step 7). The BLB constructs did not develop a necrotic core during this period of time *in vitro*. The BLB constructs were then used for implantation as a sheep ACL replacement (Step 8). BLB, bone–ligament–bone; BMSCs, bone marrow stromal cells; 3D, three-dimensional; ACL, anterior cruciate ligament. Color images available online at www.liebertonline.com/tea

positioning of the tibial and femoral tunnels and avoided locating the graft too centrally. Care was taken to avoid inadvertent injury to the posterior cruciate ligament (PCL) or the intrameniscal ligament anteriorly. Anatomic landmarks to facilitate proper tibial tunnel placement include the native ACL footprint, the PCL, the anterior horn of the lateral meniscus, and the medial tibial eminence. Miniature drill guides were used to position guide wires in the center of the tibial and femoral footprints. The femoral wire was placed through a 1 cm incision over the posterior lateral femoral condyle, at the metaphyseal flare. Cannulated reamers were used over the guidewires to fashion 5–6 mm bone tunnels. The intra-articular aperture of the tunnel was cleared with a debrider. The graft was passed through the bone tunnels with a suture attached to the proximal end of the graft. Minimal tension (< 2 lbs) was applied to the graft as the proximal and distal ends were sutured to the periosteum with the knee in 30° of flexion. Notch impingement was ruled out by direct observation and knee range of motion was checked and recorded. The joint was washed with saline and the incision closed with nylon sutures after the capsule was closed with chromic sutures. Antibiotic ointment and a dressing were applied.

During recovery, the animals were placed on a heat pad and covered with a blanket to maintain body temperature, respiration rate, and other vital signs were monitored until the animal was standing. Once standing, the animal was

moved to a pen and given access to food and water. Daily monitoring of the surgical site for infection was conducted. The sutures were removed at 14 days postsurgery.

BLB and native ACL and patellar tendon dissections

After 2, 3, 4, and 6 months of implantation, BLBs and contralateral native ACLs were dissected for morphological and mechanical analyses. Sheep were euthanized with Fatal Plus. Once the animal was confirmed to be dead by visually examining the heart rate, dissection procedures were performed. The knees were dissected, removing the skin and muscle but maintaining the ligament connections at the knee. The ACL, patellar tendon and BLB were isolated by removing all other knee ligaments. To obtain ACLs and BLBs, the tibia and femur were cut mid-bone to provide tissue for gripping during mechanical testing. To obtain patellar tendons, the patellar and tibial insertions of the patellar tendons were carefully isolated keeping the patellar tendons intact. The fat pad was then carefully removed from the patellar tendons. For mechanical testing purposes, the portions of patellar tendons that were not connected to both the tibia and the patella were carefully removed, leaving the tendon portions between patella and tibia insertions intact.

Histochemical and immunohistochemical analysis of 3D BLB constructs and native ACLs

For staining, unfixed samples were placed into TBS medium (Triangle Biological Sciences), frozen in cold isopentane, and stored at −80°C until needed. Samples were sliced to obtain cross and longitudinal sections with a cryostat at a thickness of approximately 12 μm, adhered to Superfrost Plus microscopy slides and used for staining. Sections were stained for general morphology observations with hematoxylin and eosin (H&E). Highly mineralized areas of BLB/native bone interface were de-mineralized for ~1 month in Formical-4 (Decal Chemical Corporation) before embedding in TBS medium, sectioning and staining with H&E. Immunofluorescent staining with specific antibodies was performed to detect the presence of blood vessels (anti-CD-31), nerves (anti-neural cell adhesion molecule [anti-NCAM] and anti-S-100), collagen type 1, lymphocytes, neutrophils and macrophages. Frozen sections were fixed with ice cold methanol for 10 min and rinsed 3 times with phosphate-buffered saline (PBS). Sections were blocked for 30 min with PBS-0.05% Tween20 (PBST) containing 20% calf serum (PBST-S) at room temperature. Sections were incubated overnight at 4°C with the primary antibodies diluted in PBST-S. The concentration of each of the primary antibodies was as follows: 10 μg/mL of rabbit anti-NCAM (Millipore, Temecula, CA); 10 μg/mL of rabbit anti-S-100, 10 μg/mL of rabbit antineutrophil elastase, 20 μg/mL of mouse antimacrophage (MAC387), 10 μg/mL of rabbit anti-CD8 (all from Abcam); 10 μg/mL of rabbit antimacrophage scavenger receptor (Novus Biologicals); 10 μg/mL of rabbit anti-CD31 (Abbiotec); and 5 μg/mL of rabbit anti-collagen type 1 (Chemicon International). After three washes in PBST, a 1-h room temperature incubation with Cy3-conjugated anti-mouse or anti-rabbit antibody (Jackson ImmunoResearch Lab) was used for observation. After three washes in PBST co-staining of sections with fluorescein-labeled wheat germ agglutinin (5 μg/mL; Molecular Probes) was used for general observation of the sample structure. Nuclei were stained by 5 min incubation with DAPI solution (Sigma) in PBST. The sections were examined and photographed with a Leica microscope.

Mechanical testing of BLB and native ACL and patellar tendon viscoelasticity, tensile extensibility, stiffness, and strength

Stress relaxation tests were conducted to obtain the viscoelastic responses of BLB and native ACL and patellar tendon specimens using an RSA III Dynamic Mechanical Analyzer (DMA) (TA Instruments) equipped with a 35 N load cell. Before testing, the BLB and ACL were isolated from the knee with the femur and tibia attached. Both femur and tibia were trimmed to approximately 20 mm × 20 mm × 15 mm in order to fit into the DMA grips. Care was taken to keep the soft tissue intact during the trimming process. Blue Kote Aerosol (Dr. Naylor) was sprayed onto the specimen surface for optical displacement measurement using digital image correlation as shown in Figure 11. Measurements including length, width and thickness were recorded before the tests. The DMA was controlled using TA Orchestrator software provided by TA Instruments. A Grasshopper IEEE-1394b digital camera was employed for synchronized image acquisition. The samples were subjected to two continuous load-unload cycles at constant strain rate (0.01/s) followed by stress relaxation at three different strain levels. Times, loads and synchronized camera images were recorded. During the tests, the specimens were kept in a hydrated state by dripping DPBS onto the specimen.

Uniaxial tension testing was then conducted on the BLB and ACL specimens from both operated and nonoperated animals to obtain the tensile extensibility, stiffness and strength using an MTS 810 servohydraulic test system with a 25 kN load cell. A 6 mm hole was drilled on the proximal end of the femur and the distal end of the tibia. Two 6 mm stainless steel bars were inserted into the holes drilled on the bones for attachment to the metal grips on the MTS so that the femur and tibia were fixed in a 0° of flexion angle. The grips hung into a trough to submerge the specimen in saline allowing testing in a hydrated state. Initially, there was no pretension applied along the axis of the graft. A Grasshopper IEEE-1394b digital camera was again used for synchronized image acquisition. The samples were subjected to five continuous load-unload cycles at constant strain rate followed by loading until failure and the synchronized force and image recordings were compiled using LabVIEW. ImageJ and Metamorph software were used for displacement calculation via digital image correlation analysis of the camera image data.

In vitro BLB constructs were tested using a customized tensiometer designed in our lab and a 5 N load cell as described previously.[14,15] The samples were subjected to five continuous load-unload cycles at constant strain rate followed by loading until failure and the synchronized force and image recordings were again compiled using LabVIEW. Metamorph software was used for displacement calculation via digital image correlation analysis of image data from a Basler A102fc digital video camera.

In the mechanics experiments, the secondary slope of the raw load versus particle displacement response curve

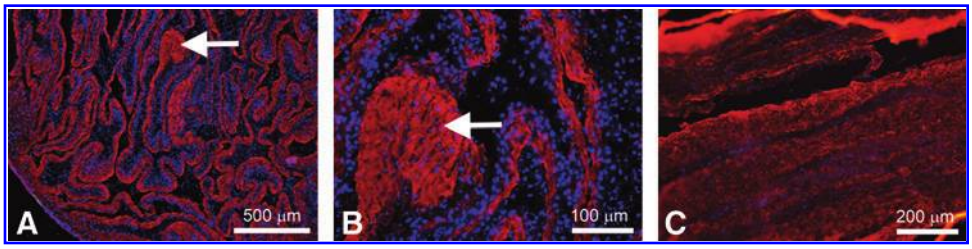

FIG. 2. Section of bone **(A, B)** and ligament **(C)** portions of BLB construct before implantation stained with antibody against collagen type 1 **(**red in **A–C)** and nuclear stain DAPI **(**blue in **A–C)**. Arrows show area of the newly formed bone with cells trapped in the collagen-rich matrix. DAPI, 4′,6-diamidino-2-phenylindole.

determined the geometric stiffness. The data were then converted to nominal stress (load/cross sectional area [CSA]) versus nominal strain (change in separation of image data/initial separation). The (maximum) tangent stiffness was determined by calculating the secondary slope of the nominal stress versus nominal strain response curve.

Results

Formation of BLB constructs in vitro

The BLB constructs were fabricated based on previously published protocols with small modifications.[14,42] Details can be found in the Methods section. Our previous studies have shown that the bone ends of the BLBs *in vitro* stain for mineralization activity (Alizarin Red). We have also shown the absence of markers for bone (Alizarin Red) and cartilage (Type II collagen) in the mid-section of the BLB constructs. Newly formed bone had areas of collagen-rich matrix with cells trapped inside the matrix (arrow in Fig. 2A, B). The mid-sections stained for type I collagen showed longitudinally oriented collagen fibers indicating fibrogenic differentiation (Fig. 2C).

Growth of BLB constructs during ACL replacement

The dimensions of the ligament portion of the *in vitro* BLB constructs before implantation ($N=7$) were approximately 30–40 mm in intra-articular length and 3.0 ± 0.2 mm in diameter ($7.1\pm1.0\,mm^2$ in CSA). The BLB constructs we have designed are viscoelastic and they contain contractile cells. Before implantation they are longitudinally constrained and carry an internal tensile stress. At the time of insertion into the bone tunnel, they undergo viscoelastic deformation to restore this passive tension. The initial compliance of the intra-articular region of the BLB graft and its ability to maintain self-tension allow it to accommodate knee motion and not slip or develop slack. The sizes and structures of adult native ACL were compared to that of our BLB explants at the time of dissection at 2-, 3-, 4-, and 6-month recovery time points (Fig. 3A–E). The native ligaments (Fig. 3F) were taken from the contralateral knees of animals at the 6-month recovery period time point. These results demonstrate that the BLB constructs rapidly grew physically in cross section during the initial implantation period and reached the size of native adult ACL at about 4 months after implantation.

Analysis of structure, vascularization, and innervation of the repaired ACL

After 6 months of implantation *in vivo*, we compared cross sections at the centers of all BLB explants with those of the native ACL. Figure 4 shows H&E staining of cross sections through the centers of our BLB explants after 6 months *in vivo* ($N=4$). Figure 4A and B show the cross sections of the BLB explants fabricated using frozen BMSCs whereas Figure 4C and D show the cross sections of the BLB explants fabricated using fresh BMSCs. In constructs made from frozen

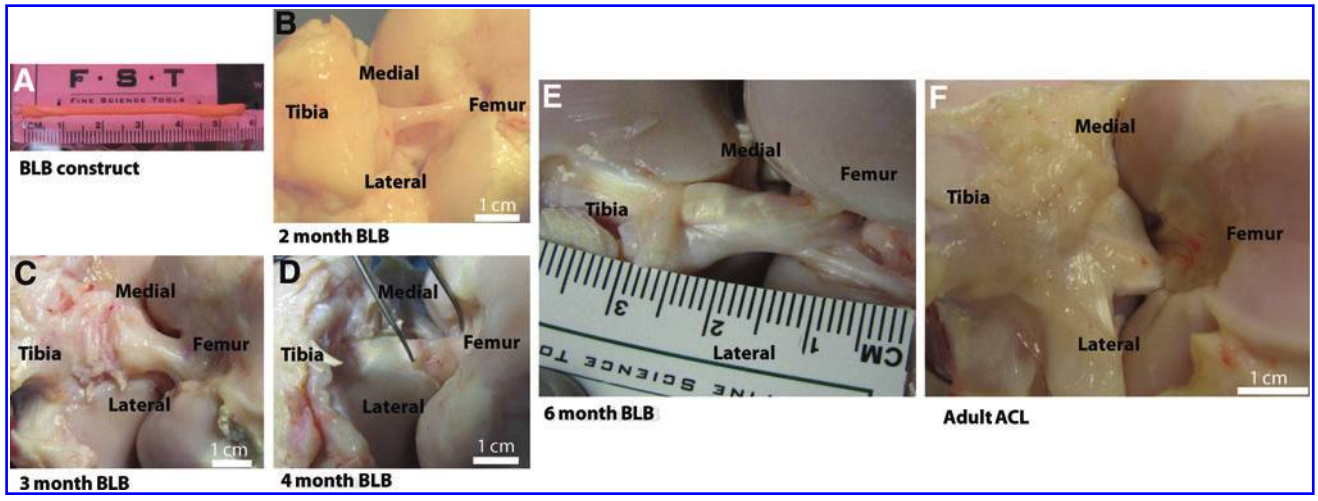

FIG. 3. BLB construct *in vitro* **(A)** 30–40 mm in intra-articular length by $7.1\pm1.0\,mm^2$ CSA, ($N=7$); BLB explant *in vivo* at **(B)** 2 months: 17 mm long by $14\,mm^2$ CSA ($N=1$), **(C)** 3 months: 18 mm long by $28\,mm^2$ CSA ($N=1$) **(D)** 4 months: 18 mm by $64\,mm^2$ CSA ($N=1$) and **(E)** 6 months: 16.3 ± 1.1 mm long by $57.5\pm48.7\,mm^2$ CSA ($N=4$); native adult ACL: 18.5 ± 0.8 mm long by $27.7\pm4.3\,mm^2$ CSA ($N=3$) **(F)**. CSA, cross sectional area. Color images available online at www.liebertonline.com/tea

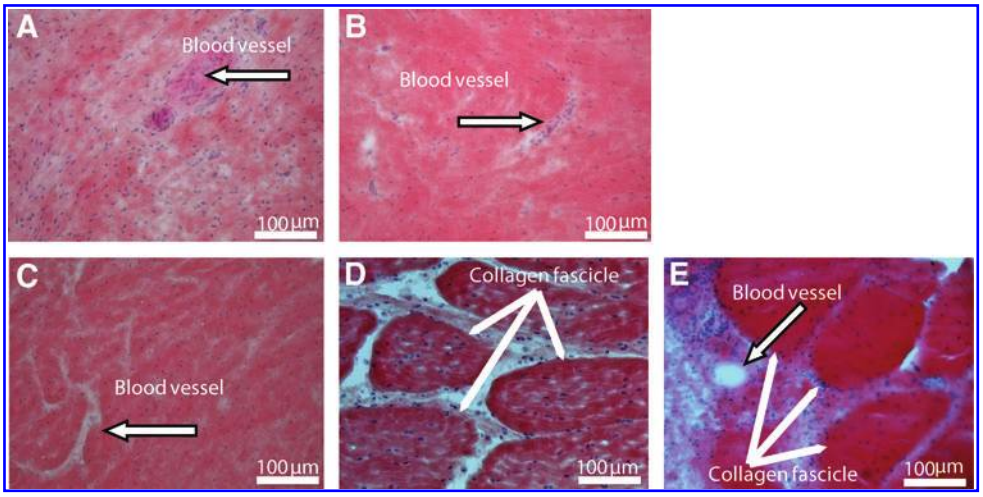

FIG. 4. H&E staining of cross-sections of BLB explants after 6 months of implantation *in vivo* as an ACL replacement **(A–D)** and of native adult ACL **(E)**. The center of section **(A, B)** made from frozen BMSCs contained viable cells and was highly vascularized (arrow) but did not have well formed collagen fascicles. The cross section **(C)** made from fresh cells suggest possible collagen fascicle formation. Explant **(D)** made from fresh cells also appeared to have fully remodeled with collagen fascicle size and structure that very closely resembled that seen in adult native ACL in **(E)**. H&E, hematoxylin and eosin. Color images available online at www.liebertonline.com/tea

cells (Fig. 4A, B), the center of the section contained viable cells and was also highly vascularized (arrow in Fig. 4A, B), suggesting that the BLB was fully viable and actively remodeling and growing but that more time was needed *in vivo* to fully fill out the section with ligament tissue. In constructs made from fresh cells (Fig. 4C), we see evidence of the initial fascicle formation. In Figure 4D (arrows) we see a fully remodeled BLB with collagen fascicle size and structure that very closely resembles that seen in adult native ACL (arrows in Fig. 4E). We analyzed frozen sections of the middle portion of the BLB explants for the presence of both blood vessels and nerves, using anti-CD31 and anti-NCAM antibody immunostaining, respectively (Fig. 5). CD31 (PECAM1) is a member of the immunoglobulin superfamily. It is a major constituent of the endothelial cell intercellular junctions and is considered to be a specific marker for blood vessels. NCAM is expressed in all neurons from very early in the development. It is considered to be a specific marker for the neuronal cell bodies, axons, and dendrites. We found, after a 3-month recovery, the midsection of the BLB-replaced ACL contained an extensive vasculature (Fig. 5B). The vasculature was greater than that observed in adult tissues and equivalent to that of a 14-day-old native neonatal sheep ACL (Fig. 6E). Additionally, we observed innervation of nerve in the midsection of the replaced ACL (Fig. 5C, F, I). After a 4-month recovery, the midsection of the replaced ACL had larger and more organized blood vessels and nerves (Fig. 5E, F) and continued further organization of blood vessels and nerves was seen after a 6-month recovery (Fig. 5H, I). H&E staining of these same explants showed more organized collagen fibers with time *in vivo* (Fig. 5A, D, G). These data suggest that our tissue-engineered BLBs remodeled *in vivo* with respect to mechanical structure (collagen alignment) and biological function as indicated by the vascularization and innervation. To compare the explants with native sheep ligaments, we stained frozen longitudinal tissue sections from 1-day, 14-day and adult sheep ACL for general structure, vascularization, and innervation (Fig. 6). The innervation and vascularization of the BLB explants at 6 months (Fig. 5H, I) *in vivo* resembles that of the adult ACL (Fig. 6H, I).

Analysis of BLB/native bone interface

Figure 7 shows a demineralized longitudinal section of a BLB explant after 2 months *in vivo* as an ACL replacement. Within 2 months as an ACL replacement in the sheep, our BLB constructs have integrated well with native tissue to form a structurally viable and biochemically relevant enthesis. Sharpey's fibers (white arrow in Fig. 7A) indicate integration of native bone with the engineered tissue. Aligned nuclei (white arrow) indicative of a fibrocartilagenous region are seen in Figure 7B.

Biomechanical stiffness and modulus analysis of BLB explants and native ACL

We conducted mechanical loading tests by prescribing a displacement ramp to a given strain level and then reversing to zero strain at the same rate (a strain-controlled load-unload tension test). The tangent modulus (the slope of the stress–strain curve at specified strain range) of the BLB explants at 6 months ($N=3$) averaged 130.0 ± 17.2 MPa (strain range: 0.10–0.35), the modulus of the contralateral ACL, 250.7 ± 8.5 MPa ($N=3$; strain range: 0.10–0.35), and the tangent modulus of ACLs from nonoperated animals was found to be 232 ± 11 MPa ($N=2$; strain range: 0.10–0.35), see Figure 8A. We also measured geometric stiffness (the slope of the load-displacement curve at specified displacement) and found 359.0 ± 150.6 N/mm for the BLB explants and 379.2 ± 73.6 N/mm for the contralateral ACL (Fig. 8B). The geometric stiffness was a function of the CSA and composition of the graft, both of which varied in the developing BLB explants at 6 months. Before implantation the BLB constructs had a tangent modulus of 1.4 ± 0.14 MPa ($N=3$; strain range: 0.2–0.3). These data indicate that after 6 months *in vivo* as an ACL replacement, the BLB constructs increased in mechanical properties by a factor of over 90 to attain 52% of the tangent modulus and 95% of the geometric stiffness of an adult contralateral ACL.

We measured the initial responses to an imposed strain of 0.15 in the BLB explants at 6 months versus the animal-matched adult contralateral ACL (Fig. 8C, D). These data

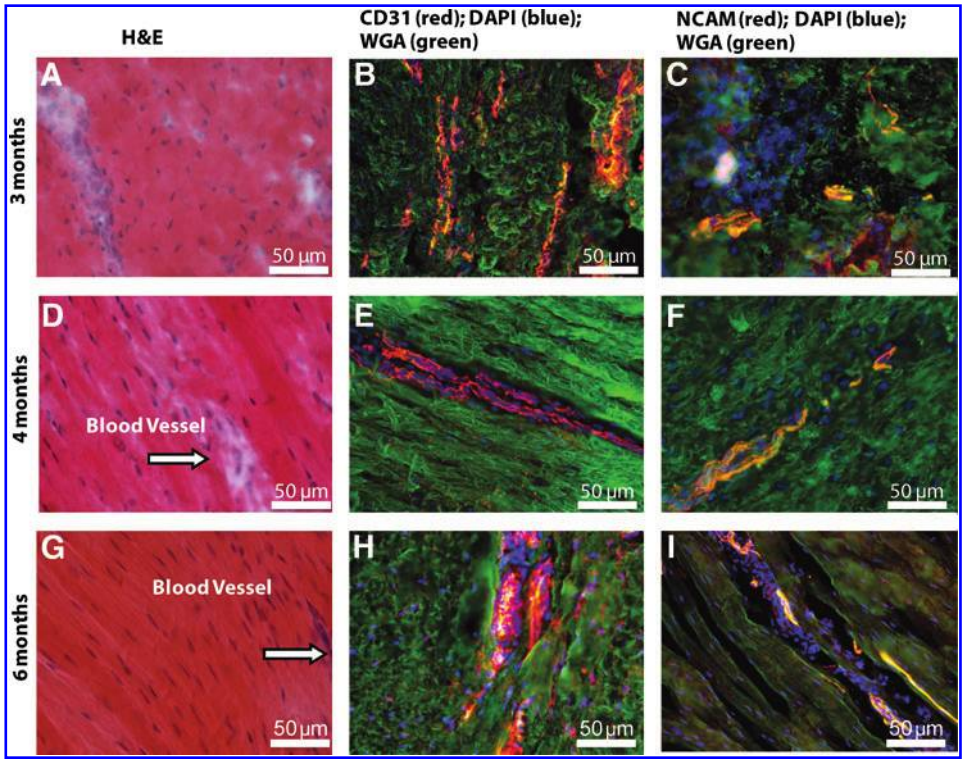

FIG. 5. Longitudinal sections of BLB explants after **(A–C)** 3, **(D–F)** 4, and **(G–I)** 6 months of implantation *in vivo* as an ACL replacement. **(A, D, G)** H&E staining for observation of general structure and collagen fibers; arrows show blood vessels found in tissue. **(B, E, H)** CD31 immunostaining for observation of blood vessels; **(C, F, I)** NCAM immunostaining for observation of nerves. NCAM, neural cell adhesion molecule; WGA, wheat germ agglutinin.

demonstrate that the initial stress–strain response of the BLB explant at 6 months is more compliant in the 0% to 10% strain range (the physiologically relevant *in vivo* range) but that the load-displacement response curves of the BLB explant and the adult contralateral ACL are quantitatively and qualitatively similar. The load-displacement results indicate that at 6 months the BLB explants are capable of carrying physiologically relevant loads, accurately matching the biomechanics of adult ACL. The stress–strain results demonstrate that the tissue of the BLB is not yet fully remodeled to that of adult ACL because the BLB is more compliant than the adult ACL. More time *in vivo* or a rehabilitation protocol may allow complete remodeling of the BLB to an adult ACL phenotype.

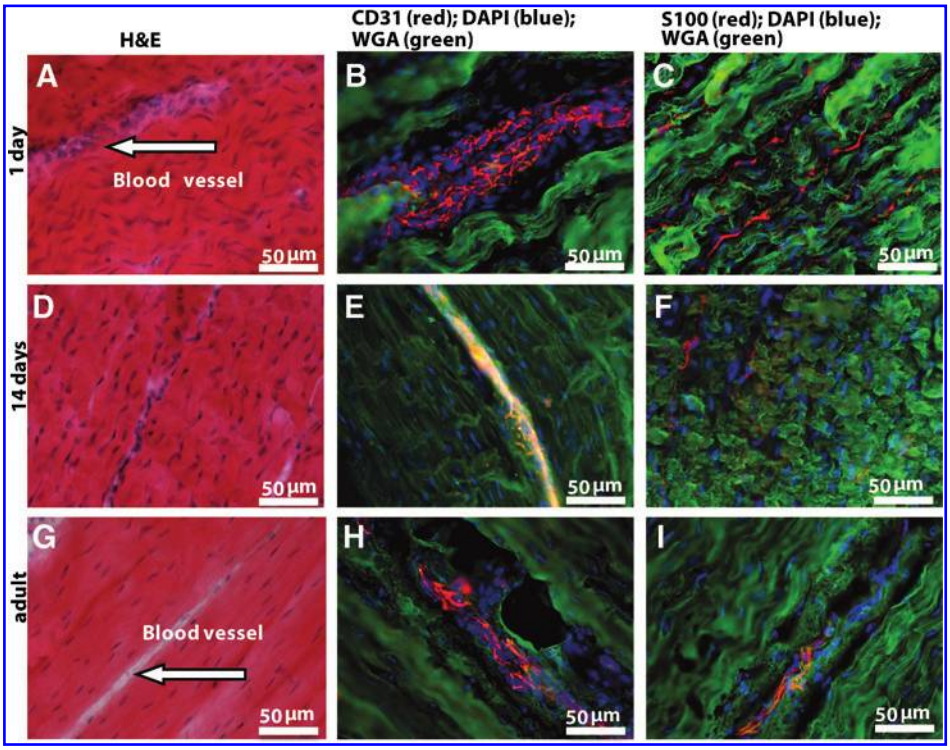

FIG. 6. Longitudinal sections of neonatal and adult native sheep ACL. Pictures of **(A–C)** 1-day-old, **(D–F)** 14-day-old and **(G–I)** adult sheep ACL are shown. **(A, D, G)** H&E staining for observation of general structure and collagen fibers; arrows show blood vessels found in tissue. **(B, E, H)** CD31 immunostaining for observation of blood vessels; **(C, F, I)** S-100 immunostaining for observation of nerves.

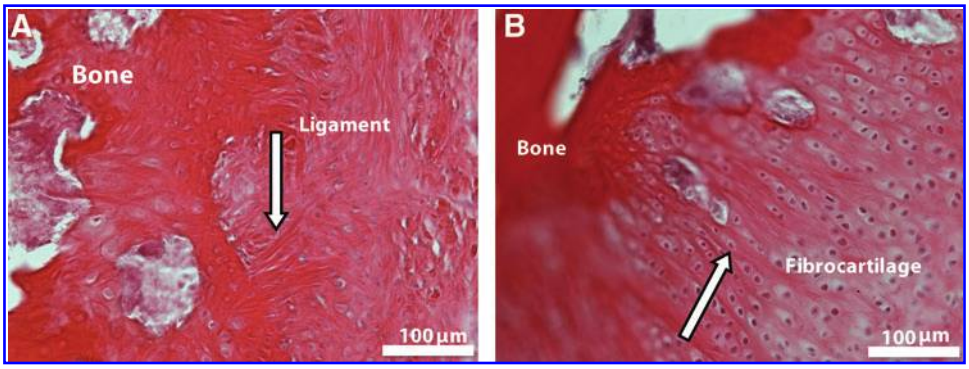

FIG. 7. BLB explant/native bone interface 2 months after implantation *in vivo* as an ACL replacement. Two sections of the BLB explant shows **(A)** integration into native bone through the Sharpey's fibers (arrow) and **(B)** fibrocartilaginous region with aligned nuclei (arrow). Color images available online at www.liebertonline.com/tea

Native ACL, native patellar tendon and BLB explant viscoelasticity

The nonlinear stress relaxation response of the BLB explants after 6 months as ACL replacements in the sheep ($N=1$) was compared to those of the native ACL in the contralateral knee ($N=1$) and to adult patellar tendons ($N=2$). The results for one animal-matched ACL and BLB pair are shown in Figure 9A and B. The stress relaxation response of the BLB explant is virtually indistinguishable from that of the contralateral ACL indicating the BLB is capable of maintaining physiologically relevant viscoelastic characteristics of adult ACL after 6 months as an ACL replacement in the sheep. The patellar tendon stress relaxation results are shown in Figure 9C to differ from those of the ACL and our BLB explants in important ways. The initial rate of patellar tendon stress relaxation increases with increased initial strain and the relaxation rate reaches a steady state at long times, whereas for the ACL and the BLB explant the rate of relaxation decreases with increased initial strain.

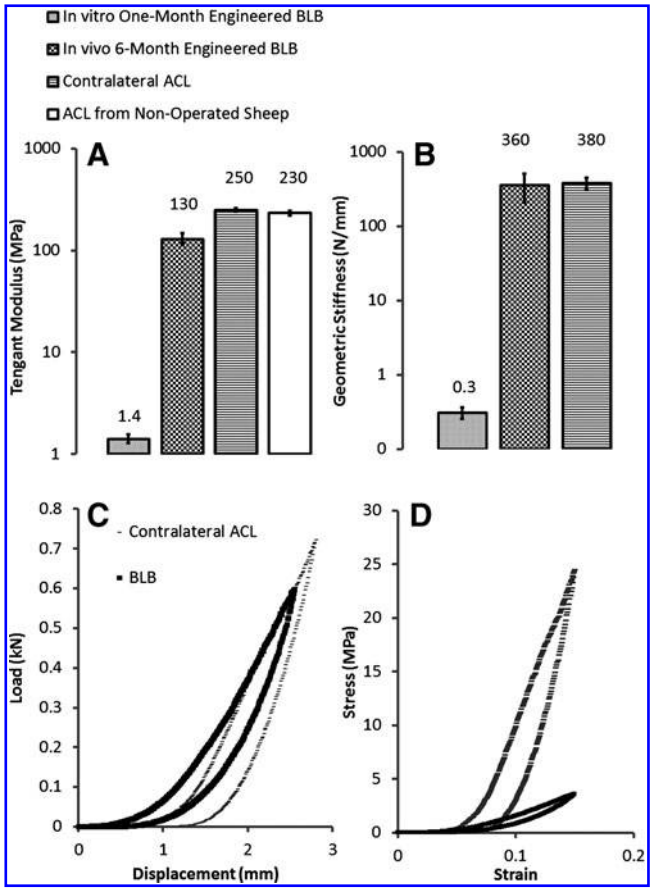

FIG. 8. Modulus and stiffness of BLB explants after 6 months of implantation and contralateral ACLs of adult sheep. **(A)** Tangent modulus of the linear portion of the stress–strain response curves over a strain range of 0.10–0.35. **(B)** Corresponding geometric stiffness **(C)** Stress–strain relationship and **(D)** Load-displacement curves detailing the initial responses (physiological or <5% strain) of BLB explants and adult contralateral ACLs.

Strength of bone/graft and bone/ACL complexes

Three BLB explants at 6 months and contralateral ACLs were loaded until failure after completion of the load-unload and stress relaxation experiments. In all cases failure occurred by failure of the tibia in the grip of the testing system; therefore, no failure loads can be recorded for our BLB explants or the contralateral ACLs. However, the maximum loads before bone failure in the grips occurred were recorded and the average values are 676.3 ± 356.4 N ($N=3$) for the BLB explants and 970.7 ± 384.1 N ($N=3$) for the contralateral ACLs. The maximum loads expected *in vivo* are conservatively estimated at 250 N (the load at 10% strain). Although BLB strengths could not be determined, they clearly exceed the *in vivo* loads. All of the seven implanted BLB constructs integrated with native bone, and all survived the implantation experiments intact.

Native ACL and patellar tendon moduli

We conducted mechanical loading tests by prescribing a displacement ramp to a given strain level and then reversing to zero strain at the same rate (a strain-controlled load-unload tension test). These load-unload experiments were conducted on animal-matched ACLs and patellar tendons of 2-month-old ($N=2$) and adult ($N=1$) sheep (Fig. 10). Both tissues exhibit nonlinear viscoelasticity with hysteresis in the load-unload response. At small strains the stress–strain response curves of the patellar tendon and ACL diverge and the patellar tendon is seen to have a higher tangent modulus (slope of the stress–strain loading curve as shown for example by the gray line segments in Fig. 10) at all strain levels beyond 0.002 (0.2%). These data are in agreement with recent data on patient-matched human ACLs and patellar tendons, which also demonstrated a greater tangent modulus for the patellar tendon.[17]

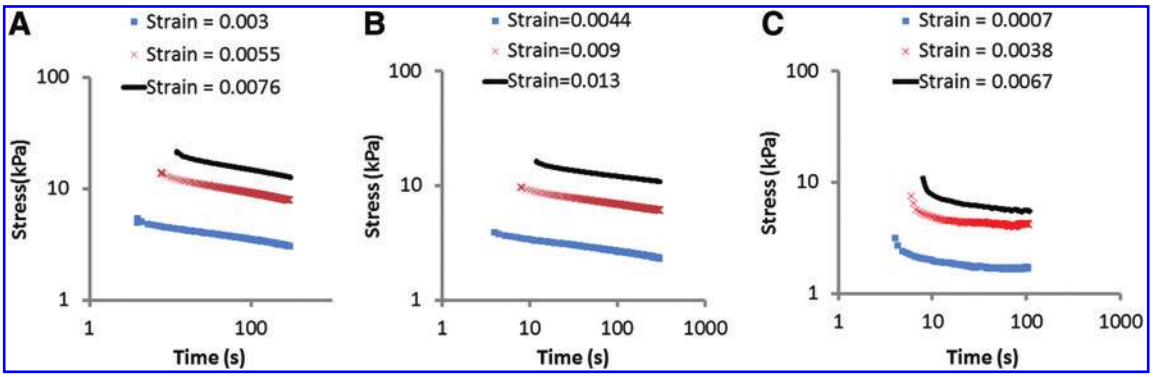

FIG. 9. Stress relaxation as a function of initial strain for animal-matched **(A)** ACL and **(B)** BLB explant in adult sheep and **(C)** adult patellar tendon. Color images available online at www.liebertonline.com/tea

Analysis of body fluids and tissue sections for signs of immune rejection

Samples of blood (3 months) urine (3 months) and synovial fluid (3, 4, and 6 months) were obtained before dissection from ACL repaired and contralateral (control) knees. These were analyzed for an increase in white blood cell count and the presence of neutrophils and macrophages as indicators of an infection and a mounted immune response against the implanted tissue. The hematology, urinalysis reports and histological analysis of synovial fluid were unremarkable and showed no indications of infection or immune rejection in these animals. During dissection, portions of the engineered ligament were frozen, subsequently sectioned and stained for the presence of neutrophils and macrophages. We did not detect the presence of neutrophils or macrophages in any of the BLB grafts examined. Sections of spleen were used as a positive control.

Discussion

We have developed a multi-phasic, engineered BLB construct with a viable, intact bone–ligament interface *in vitro* and the capacity to become vascularized and innervated when implanted in sheep, with complete ligamentization and mechanical properties comparable to those of adult ACL. Our multi-phasic engineered ligament and bone tissues can be fabricated from an autogenic source but without the donor site morbidity associated with patellar tendon and hamstring autografts. Tissue availability is not a limiting factor with this approach due to a plentiful and easily accessible allogenic cell source as well. The lack of immune rejection of our constructs after implantation indicates that allogenic rather than autogenic sources of BMSCs may be used.

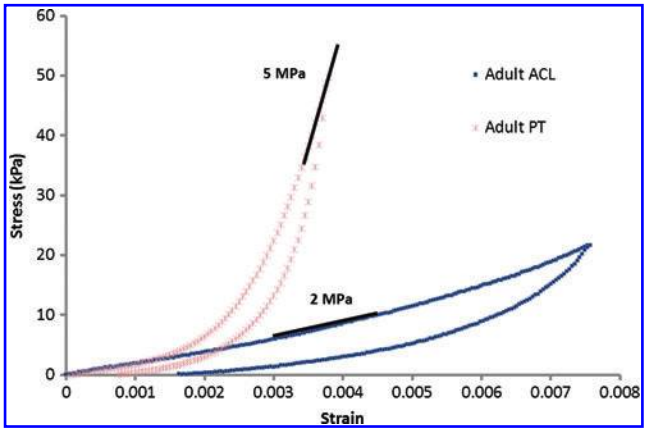

FIG. 10. Stress–strain response curves of a patellar tendon and an ACL from the same animal. Color images available online at www.liebertonline.com/tea

The elasticity requirements of engineered ligament at the time of replacement remain under debate.[20,43–45] The current paradigm is to match or exceed native ligament stiffness and strength in order to immediately restore stability to the knee.[44] However, recent evidence suggests stiff scaffolds shield the cells within these structures from strains required for proper signal induction and, hence, growth of neoligamentous tissue.[20,44,45] The result is loss of cell viability with time *in vivo* and increased joint laxity.[43,45] Moreover, the stresses during normal ACL function do not typically exceed 20% of ACL strength[43] suggesting that current engineering approaches are over-designed for strength, especially if eventual collagen growth and remodeling is expected with time. Therefore, an engineered ligament that is compliant upon implantation such that its cells are not strain shielded would promote cell growth, remodeling of tissues and eventual ligamentization. In our approach, the animals were not restrained during healing. During the early healing period, the BLB implants do not need to sustain a physiological load, they need to be able to accommodate knee motion without tearing. Because our BLBs are compliant initially, they can sustain a physiological length change during knee motion. Also, because they are viscoelastic, they recover that length change upon unloading. The BLB constructs were fabricated at a slightly larger length than the expected intra-articular span and at the time of implantation the ends of the bone sections were aligned with the insertion edges of the bones, allowing the intra-articular region to quickly (within seconds) retension itself, providing a perfect patient-specific fit. This allowed us to fabricate one size construct for any size knee.

Current ACL grafts often do not fully heal at the bone tunnel even after 2 years and may display joint laxity and graft failure.[46,47] In contrast we have established very rapid (within 2 months) integration of the constructs with native

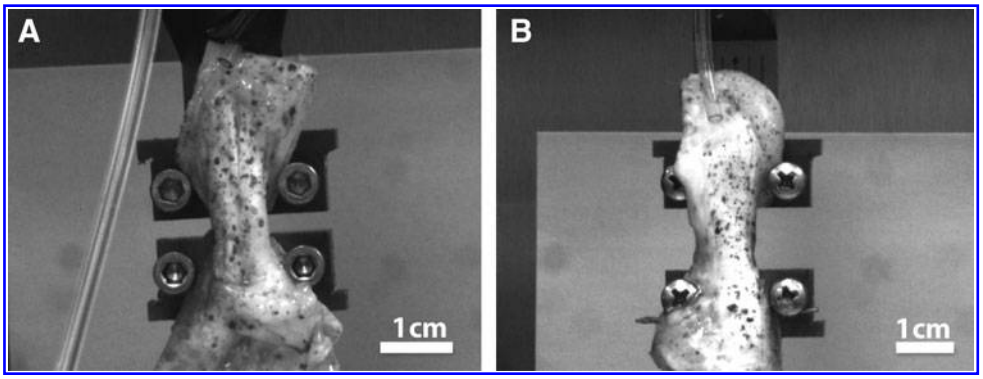

FIG. 11. RSA III Dynamic Mechanical Analyzer evaluation of stress relaxation. evaluation of **(A)** BLB explant and adult contralateral **(B)** ACL.

bone (Fig. 7) and healing of our multi-phasic BLB constructs in the bone tunnel (see Fig. 3B–E). Therefore, the need to protect our grafts in the bone tunnel (i.e., by delayed or mild physical therapy or via metal fixation screws) is diminished. Well-integrated bone ends allowed rapid growth *in vivo* (within 3 months) of vascularization and innervation *in vivo*. After 6 months of *in vivo* recovery, we have shown that the BLB grafts can sustain very large loads, well-beyond physiological limits, and also the same load magnitudes that the contralateral ACLs can withstand. The average CSA of the *in vivo* BLB $57.5 \pm 48.7\,mm^2$ and the CSA of the contralateral ACL is $27.7 \pm 4.3\,mm^2$. The initial CSA of the BLBs before the surgery is $7.1 \pm 1.0\,mm^2$. The size of the bone tunnel needed to accommodate the BLB graft was less than that typically used clinically (see Methods section). Our results suggest the thinner bone tunnel may heal faster and it may accelerate the growth and remodeling of the BLBs. Therefore, the implication of BLBs increasing in size *in vivo* over time is significant. We demonstrate that a full-sized graft is not needed if it can develop rapidly *in vivo*. Statistically, the 6 month *in vivo* BLB is not significantly larger than native ACL. The large standard deviation is due to the large CSA of one BLB explant. At present, the issue of overgrowth of the BLB is not of concern. At each time point examined thus far (2, 3, 4, and 6 months), the issue of growth and size has not been a negative factor. The ligaments have fit well into the femoral notch and do not appear to be growing disproportionally.

At 6 months *in vivo* the vascularization of the BLB closely resembled that of the adult ACL. Vascularization is a process essential to growth and remodeling of our BLB construct. During regeneration of the injured ligament, pathways for repair are similar to those observed during development, as indicated by our analysis of developing sheep at one day, 14 days and adult to compare our regenerating tissue to those of developing ACL, enthesis and bone (Figs. 6 and 7). The development of the BLB appears to recapitulate the developmental processes observed in developing native ACL.

A human ACL can sustain a load of 2000 N before rupturing.[48] Some investigators believe that the ability to withstand such loads without rupture during extension of the knee is due to activation of an ACL-hamstring reflex arc and subsequent contraction of the hamstrings muscles that counterbalances the forces of the quadriceps on the tibia and prevents the rupture of the ACL.[35] This reflex arc is destroyed during the severing of the ACL and is usually not reinnervated with patellar or hamstring tendon grafts. While the contribution of the ACL-hamstrings reflex arc to proprioception and its role in the prevention of ACL rupture is controversial,[49,50] the functional innervation observed in some models of repair will only further enhance the recovery potential of the ACL.[49,50] In our BLB grafts, we have observed innervation of the grafts as early as 3-months after implantation (see Fig. 6), although we do not yet know whether this innervation is functional. Ongoing studies in our laboratory are investigating the return of the ACL elicited electromyography activity in the hamstrings muscle and the recovery of native kinematics as a results of the observed innervation.

The tangent modulus of ACLs from nonoperated animals was found to be 232 ± 11 MPa ($N = 2$). The moduli of nonoperated animals were not significantly different from those of the contralateral ACLs from operated animals. We have compared our modulus results with values from literature.[38–40] The reported geometric stiffness values for sheep ACL were converted to tangent moduli using the geometric properties provided[38–40] and the average value found to be 130 ± 15 MPa. This value is lower than our results and the differences are due to the fact that we measure the actual tissue level displacement directly and noninvasively whereas the literature results recorded the grip-to-grip displacement that neglected the compliance within the system and nonphysiological issues associated with mechanical testing such as slip, tearing and stress concentrations at the grips.

The patellar tendon autograft is a common source of tissue for ACL repair. Recently the biomechanical properties of the ACL and the patellar tendon have been compared within the physiological range of 5% strain[16,17] and the results suggest that current ACL grafts are often over-designed for stiffness (Fig. 10). Our multi-phasic constructs rapidly increased stiffness and strength *in vivo* in response to stresses and strains placed on them to attain physiologically relevant mechanics. We believe the initial compliance of the intra-articular region of the graft allowed the graft to strain at relatively low stress levels. This deformability was conducive to mechanotransduction of the cells within the intra-articular region. It had the added benefit of transferring very low loads to the regions of the graft within the bone tunnels in the weeks after surgery during which bone tunnel healing occurs, eliminating the need for metal fixation screws to hold the graft in place. At 6 months as an ACL replacement in the sheep some of the BLB grafts contained fascicles of type I collagen that were highly aligned and resembled the collagen fascicle structure and alignment of native adult ACL.

Moreover, native ACL has a characteristic viscoelastic relaxation response that is not shared by patellar tendon grafts; our multi-phasic BLB constructs did exhibit qualitatively and quantitatively similar stress relaxation responses to those of native ACL. These results indicate that the patellar tendon is not an ideal biomechanical replacement for the ACL, not only because it is too stiff, but also because its time dependent properties are very different at the time of implantation from those of native ACL. This has important implications for the risk of re-injury when using a patellar tendon graft, especially at high strain rates of loading such as in an impact event, because the viscoelastic or time dependent properties govern the high strain rate response. It is not known whether the patellar tendon graft develops and maintains the proper viscoelastic response over time, but it is clear that its viscoelastic response is initially fundamentally different from that of native ACL. The relevance of the patellar tendon data is that it isn't biomechanically similar to ACL despite the fact that the patellar tendon is adult, native connective tissue. The goal is also to establish that the BLB constructs have the proper nonlinear viscoleastic properties compared to those of native tissue which are not matched by current ACL repair techniques utilizing patellar tendon grafts. This result has the further significance of addressing how arduous a task it is to accurately match the very important nonlinear viscoelastic properties of the native ACL with a graft-engineered or otherwise.

Tissue engineering grafts for ACL repair has been increasingly focused recently. For instance, Cooper *et al.* (2007) has developed synthetic braided scaffolds as grafts for ACL repair.[51] Synthetic scaffolds are not needed in our method. One of the disadvantages of using synthetic scaffold is that its degradation rates *in vivo* often exceed the desired rates. Infiltration of collagen fibers are seen in these types of scaffolds *in vivo*; however, the overall mechanical properties decrease rapidly over time because of the rapidly biodegrading scaffold. On the other hand, our scaffold-less self-assembled BLB grafts grow rapidly *in vivo* and the mechanics of the *in vivo* BLB have increased a factor of 90 compared to that of the *in vitro* BLB before the implantation. In addition, the integration of ends to native bone was not evaluated in Cooper *et al*. (2007). There is no evidence showing that the synthetic graft formed a strong enthesis between the graft and the native bone, whereas our BLB has shown markers of enthesis early after 2 months of implantation.

In conclusion, the biomechanical requirements of an ACL graft at the time of implantation were examined with the aim of developing an engineered ACL graft that would rapidly grow and remodel *in vivo* to present the histological and biomechanical characteristics of adult, native ACL. We have demonstrated that our BLB constructs, with their initially compliant intra-articular region, do not require fixation screws to achieve a rapid *in vivo* interface with native bone, become vascularized and innervated. Some of the BLB constructs develop highly organized collagen fascicles and after 6 months *in vivo*, exhibit physiologically relevant viscoelastic properties of adult ACLs. The viscoelastic properties of an ACL graft have been largely overlooked previously but they are a critical aspect of the restoration of biomechanical function to prevent graft failures. Our ongoing studies will compare the nonlinear viscoelastic characteristics of BLB grafts to patellar tendon autografts at longer recovery time points.

Acknowledgments

EMA gratefully acknowledges support from the Michigan Institute for Clinical & Health Research through grant number UL1RR024986. T.Y.K. was supported by funds from IUSM-Northwest.

Disclosure Statement

No competing financial interests exist.

References

1. The American Orthopaedic Society for Sports Medicine Conference on Allografts in Orthopaedic, Sports Medicine. Keystone, CO, July 14–17, 2005.
2. Louw, Q.A., Manilall, J., and Grimmer, K.A. Epidemiology of knee injuries among adolescents: a systematic review. British J Sports Med **42,** 2, 2008.
3. Ingram, J.G., Fields, S.K., Yard, E.E., and Comstock, R.D. Epidemiology of knee injuries among boys and girls in US high school athletics. Am J Sports Med **36,** 1116, 2008.
4. Salgado, A.J., Coutinho, O.P., and Reis, R.L. Bone Tissue engineering: state of the art and future trends. Macro Biol **4**, 743, 2004.
5. Roos, E.M. Joint injury causes knee osteoarthritis in young adults. Curr Opin Rheum **17,** 195, 2005.
6. Wilder, F.V., Hall, B.J., Barrett, J.P., Jr., and Lemrow, N.B. History of acute knee injury and osteoarthritis of the knee: a prospective epidemiological assessment. Osteoarthritis Cartilage **10,** 611, 2002.
7. National Center for Health Statistics, National Ambulatory Medical Care Survey. 2004. American Association of Orthopaedic Surgeons. Available at aaos.org.
8. Moffat, K.L., Sun, W-H. S., Pena, P.E., Chahine, N.O., Doty, S.B., Ateshian, G.A., Hung, C.T., and Lu, H. Characterization of the Mechanical Properties and Mineral Distribution of the Anterior Cruciate Ligament-to-Bone Insertion Site. Proceedings of the 28th IEEE EMBS Annual International Conference, Vol. 1–15. New York, NY. 2006, p. 6097.
9. Moffat, K.L., Sun, W.-H. S., Pena, P.E., Chahine, N.O., Doty, S.B., Ateshian, G.A., Hung, C.T., and Lu, H. Characterization of the structure-function relationship at the ligament-to-bone interface. Proc Natl Assoc Sci **105,** 7947, 2008.
10. Scheffler, S.U., Unterhauser, F.N., and Weiler, A. Graft remodeling and ligamentization after cruciate ligament reconstruction. Knee Surg Sports Traumatol Arthrosc **16,** 834, 2008.
11. Van Porat, A., Roos, E.M., and Roos, H. High prevalence of osteoarthritis 14 years after an anterior cruciate ligament tear in male soccer players: a study of radiographic and patient relevant outcomes. Ann Rheum Dis **63,** 269, 2004.
12. Kessler, M.A., Behrend, H., Henz, S., Stutz, G., Rukavina, A., and Kuster, M.S. Function, Osteoarthritis and Activity after ACL-Rupture: 11 Years Follow-Up Results of Conservative versus Reconstructive Treatment. Knee Surg Sports Traumatol Arthrosc **16,** 442, 2008.
13. Lohmander, L.S., Ostenberg, A., Englund, M., and Roos, H. High prevalence of knee osteoarthritis, pain and functional limitations in female soccer players twelve years after anterior cruciate ligament injury. Arthritis Rheum **50,** 3145, 2004.

14. Ma, J., Goble, K., Smietana, M.J., Kostrominova, T., Larkin, L.M., and Arruda, E.M. Morphological and functional characteristics of three-dimensional engineered bone–ligament–bone constructs following implantation. J Biomech Eng **131,** 101017, 2009.
15. Ma, J., Narayanan, H., Garikipati, K., Grosh, K., and Arruda, E.M. Experimental and Computational Investigation of Viscoelasticity of Native and Engineered Ligament and Tendon. In: Garikipati, K., and Arruda, E.M., eds., Proceedings of the IUTAM Symposium on Cellular, Molecular and Tissue Mechanics, Vol. 16. Woods Hole, MA: Springer, 2010, p. 3.
16. Danto, M.I. and Woo, S.L.-Y. The mechanical properties of skeletally mature rabbit anterior cruciate ligament and patellar tendon over a range of strain rates. J Orthop Surg **11,** 58, 1993.
17. Chandrashekar, N., Hashemi, J., Slauterbeck, J., and Beynnon, B.D. Low-load behavior of the patellar tendon graft and its relevance to the biomechanics of the reconstructed knee. Clin Biomech **23,** 918, 2008.
18. Goh, J. C-H., Ouyang, H.W., and Teoh, S.H. Tissue-engineering approach to the repair and regeneration of tendon and ligaments. Tissue Eng **9**, s31, 2003.
19. Wang, I-N. E., Shan, J., Choi, R., Oh, S., Kepler, C.K., Chen, F.H., and Lu, H.H. Role of osteoblast-fibroblast interactions in the formation of the ligament-to-bone interface. J Orthop Res **25,** 1609, 2007.
20. Petrigliano, F.A., McAllister, D.R., and Wu, B.M. Tissue engineering for anterior cruciate ligament reconstruction: a review of current strategies. Arthroscopy **22,** 441, 2006.
21. Ge, Z., Yang, F., Goh, J.C.H., Ramakrishna, S., Lee, E.H. Biomaterials and scaffolds for ligament tissue engineering. J Biomed Mater Res Part A **77A,** 639, 2006.
22. Bernardino, S. ACL prosthesis: any promise for the future? Knee Surg Sports Traumatol Arthrosc **18,** 794, 2010.
23. Kuo, C.K., Marturano, J.E., Tuan, R.S. Novel strategies in tendon and ligament tissue engineering: Advanced biomaterials and regeneration motifs. Sports Med Arthrosc Rehabil Ther Technol **2**, 20, 2010.
24. Caplan, A. Adult mesenchymal stem cells for tissue engineering versus regenerative medicine. J Cell Physiol **213,** 341, 2007.
25. Alhadlaq A., and Mao, J.J. Mesenchymal stem cells: isolation and therapeutics. Stem Cell Dev **13,** 436, 2004.
26. Pittenger, M.F., Mackay, A.M., Beck, S.C., Jaiswal, R.K., Douglas, R., Mosca, J.D., Moorman, M.A., Simonetti, D.W., Craig, S., and Marshak, D.R. Multilineage potential of adult human mesenchymal stem cells. Science **284,** 143, 1999.
27. Dezawa, M., Ishikawa, H., Itokazu, Y., Yoshihara, T., Hoshino, M., Takeda, S., Ide, C., and Nabeshima, Y. Bone marrow stromal cells generate muscle cells and repair muscle degeneration. Science **309,** 314, 2005.
28. Moreau, J.E., Chen, J.S., Bramono, D.S., Volloch, V., Chernoff, H., Vunjak-Novakovic, G., Richmond, J.C., Kaplan, D.L., and Atlman, G.H. Growth factor induced fibroblast differentiation from human bone marrow stromal cells in vitro. J Orthop Res **23,** 164, 2005.
29. Kretlow, J.D., Jin, Y-Q., Liu, W., Zhang, W.J., Hong, T-H., Zhou, G., Baggett, L.S., Mikos, A.G., and Cao, Y. Donor age and cell passage affects differentiation potential of murine bone marrow-derived stem cells. BMC Cell Biol **9**, 60, 2008.
30. Nirmalanandhan, V.S., Juncosa-Melvin, N., Shearn, J.T., Biovin, G.P., Galloway, M.T., Gooch, C., Bradica, G., and Butler, D.L. Combined effects of scaffold stiffening and mechanical preconditioning cycles on construct biomechanics, gene expression and tendon repair biomechanics. Tissue Eng **15,** 2103, 2009.
31. Woo, S. L-Y., Liang, R. and Fisher, M.B. Future of orthopaedic sports medicine and soft tissue healing: the important role of engineering. Cell Mol Bioeng **2,** 448, 2009.
32. Lundberg, W.R., Lewis, J.L., Smith, J.J., Lindquist, C., Meglitsch, T., Lew, W.D., and Poff, B.C. In vivo forces during remodeling of a two-segment anterior cruciate ligament graft in a goat model. J Orthop Res **15,** 645, 1997.
33. Singhatat, W., Lawhorn, K.W., Howell, S.M., and Hull, M.L. How four weeks of implantation affect the strength and stiffness of a tendon graft in a bone tunnel: a study of two fixation devices in an extraarticular model in ovine. Am J Sports Med **30,** 506, 2002.
34. Radford, W.J.P., Amis, A.A., and Stead, A.C. The ovine stifle as a model for human cruciate ligament surgery. Vet Comp Orthop Trauma **9,** 134, 1996.
35. Tapper, J.E., Ronsky, J.L., Powers, M.J., Sutherland, C., Majima, T., Frank, C.B., and Shrive, N.G. In vivo measurement of the dynamic 3-D kinematics of the ovine stifle joint. J Biomech Eng **126,** 301, 2004.
36. Seitz, H., Hausner, T., Schlenz, I., Lang, S., and Eschberger, J. Vascular anatomy of the ovine anterior cruciate ligament. A macroscopic, histological and radiographic study. Arch Orthop Trauma Surg **116,** 19, 1997.
37. Murray, M.M., Weiler A., and Spindler, K.R. Interspecies variation in the fibroblast distribution of the anterior cruciate ligament. Am J Sports Med **32,** 1484, 2004.
38. Dustmann, M., Schmidt, T., Gangey, I., Unterhauser, F.N., Weiler A., and Scheffler, S.U. The extracellular remodeling of free-soft-tissue autografts and allografts for reconstruction of the anterior cruciate ligament: a comparison study in a sheep model. Knee Surg Sports Traumatol Arthrosc **16,** 360, 2008.
39. Hunt, P., Scheffler, S.U., Unterhauser F. N., and Weiler, A. A model of soft-tissue graft anterior cruciate ligament reconstruction in sheep. Arch Orthop Trauma Surg **125,** 238, 2005.
40. Meller, R., Willbold, E., Hesse, E., Dreymann, B., Fehr, M., Haasper, C., Hurschler, C., Krettek, C., and Witte, F. Histologic and biomechanical analysis of anterior cruciate ligament graft to bone healing in skeletally immature sheep. Arthroscopy **24,** 1221, 2008.
41. Dürselen, L., Claes, L., Ignatius, A., and Rubenacker, S., Comparative animal study of three ligament prostheses for the replacement of the anterior cruciate and medial collateral ligament. Biomaterials **17,** 977, 1996.
42. Syed-Picard, F.N., Larkin, L.M., Shaw, C.M., and Arruda, E.M. Engineered functional bone from bone marrow stromal cells and their autogenous extra-cellular matrix. Tissue Eng **15,** 187, 2009.
43. Frank, C.B., and Jackson, D.W. The science of reconstruction of the anterior cruciate ligament. J Bone Joint Surg Am **79,** 1556, 1997.
44. Freeman, J.W., Woods, M.D., and Laurencin, C.D. Tissue engineering of the anterior cruciate ligament using a braid-twist scaffold design. J Biomech **40,** 2029, 2007.
45. Mascarenhas, R., and MacDonald, P.B., Anterior Cruciate ligament reconstructions: a look at prosthetics–past, present and possible future. McGill J Med **11,** 29, 2008.
46. Salmon, L.J., Russell, V.J., Refshauge, K., Kader, D., Connolly, C., Linklater J., and Pinczewski, L.A. Long-term outcome of endoscopic anterior cruciate ligament reconstruction

with patellar tendon autograft. Am J Sports Med **34,** 721, 2006.
47. Ait Si Selmi, T., Fithian, D., and Neyret, P. The evolution of osteoarthritis in 103 patients with ACL reconstruction at 17 years follow-up. Knee **13,** 353, 2006.
48. Krogsgaard, M.R., Dyhre-Poulsen, P., and Fischer-Rasmussen, T. Cruciate ligament reflexes. J Electromyogr Kinesiol **12,** 177, 2002.
49. Palmieri-Smith, R.M., and Thomas, A.C. A neuromuscular mechanism of posttraumatic osteoarthritis associated with ACL injury. Exerc Sport Sci Rev **37,** 147, 2009.
50. Wojtys, E.M., and Huston, L.J. Neuromuscular performance in normal and anterior cruciate ligament-deficient lower-extremities. Am J Sports Med **22,** 89, 1994.
51. Cooper, J.M., Sahota, J.S., Gorum, W.J., II, Carter, J., Doty, S.B., and Laurencin, C.T. Biomimetic tissue-engineered anterior cruciate ligament replacement. Proc Natl Acad Sci **104,** 3049, 2007.

Address correspondence to:
Ellen M. Arruda, Ph.D.
Departments of Mechanical Engineering
and Biomedical Engineering
University of Michigan
3126 GG Brown
Ann Arbor, MI 48109

E-mail: arruda@umich.edu

Received: April 21, 2011
Accepted: July 18, 2011
Online Publication Date: September 23, 2011

This article has been cited by:

1. Jessica M. Deneweth, Kelly E. Newman, Stephen M. Sylvia, Scott G. McLean, Ellen M. Arruda. 2013. Heterogeneity of tibial plateau cartilage in response to a physiological compressive strain rate. *Journal of Orthopaedic Research* **31**:3, 370-375. [CrossRef]
2. Matthew B. Fisher, Robert L. Mauck. 2013. Tissue Engineering and Regenerative Medicine: Recent Innovations and the Transition to Translation. *Tissue Engineering Part B: Reviews* **19**:1, 1-13. [Abstract] [Full Text HTML] [Full Text PDF] [Full Text PDF with Links]
3. Bart Muller, Karl F. Bowman, Asheesh Bedi. 2013. ACL Graft Healing and Biologics. *Clinics in Sports Medicine* **32**:1, 93-109. [CrossRef]
4. Caglar Yilgor, Pinar Yilgor Huri, Gazi Huri. 2012. Tissue Engineering Strategies in Ligament Regeneration. *Stem Cells International* **2012**, 1-9. [CrossRef]